DOI: 10.1002/ejic.200600551

Structural Studies of $[CpMoL_2(CO)_2]^+$ (L = NCMe, L_2 = 2,2′-biimidazole) Complexes and Their Inclusion Compounds with Cyclodextrins

Cláudia C. L. Pereira,[a] Susana S. Braga,[a] Filipe A. Almeida Paz,[a] Martyn Pillinger,[a] Jacek Klinowski,[b] and Isabel S. Gonçalves*[a]

Keywords: Cyclodextrins / Inclusion compounds / Half-sandwich complexes / Molybdenum / Cyclopentadienyl metal carbonyls

Protonation of $[CpMo(\eta^3\text{-}C_3H_5)(CO)_2]$ followed by addition of acetonitrile or 2,2′-biimidazole (H_2biim) gave the complexes $[CpMo(NCMe)_2(CO)_2](BF_4)$ (**1**) and $[CpMo(H_2biim)(CO)_2](BF_4)$ (**2**) in good yields. The structures of **1** and **2** were determined by single-crystal X-ray diffraction in the orthorhombic *Pbca* and triclinic $P\bar{1}$ space groups, respectively. Both complexes have similar metal ion coordination environments, which can be envisaged as slightly distorted pseudo-square pyramids, a coordination geometry commonly compared with a four-legged piano stool. The two complexes were immobilised in native and permethylated β-cyclodextrins (β CD and TRIMEB) by methods tailored according to the stabilities and solubilities of the individual components and this gave four adducts with a 1:1 host/guest stoichiometry. The formation of true inclusion compounds was supported by powder X-ray diffraction (XRD), thermogravimetric analysis (TGA), $^{13}C\{^1H\}$ CP/MAS NMR and FTIR spectroscopy. In the case of the TRIMEB adduct containing complex **1**, the crystal packing arrangement is markedly similar to that previously reported for the corresponding 1:1 TRIMEB adducts of the neutral guests $[CpMoX(CO)_3]$ (X = Cl, CH_2CONH_2), featuring columns in which the macrocycles are arranged along the *b* axis in a tilted fashion.

Introduction

Half-sandwich metal carbonyl compounds bearing cyclopentadienyl (Cp = $\eta^5\text{-}C_5H_5$) and η^6-arene groups have been, and continue to be, investigated for applications in various fields such as catalysis,[1] nonlinear optics[2] and medicine.[3] The bioorganometallic chemistry of these compounds is of particular interest, especially in relation to their use as pharmaceuticals. For example, technetium and rhenium tricarbonyl complexes with derivatised cyclopentadienyl ligands have been investigated for radiopharmaceutical applications in the diagnosis (^{99m}Tc) and treatment (^{188}Re and ^{186}Re) of cancer.[4] In these compounds it is the radioactive metal centre that provides the activity, although the ligands attached to the metal centre will ultimately determine the selectivity and efficiency of these compounds towards target diseased cells. Considering the known antitumour action of metallocenes such as Cp_2TiCl_2 and Cp_2MoCl_2,[5] it is also possible that half-sandwich metal carbonyl compounds containing nonradioactive elements may exhibit anticancer properties. These studies are, however, in their infancy. Researchers have also examined metal carbonyls for applications that directly involve the CO ligands. One of these is their potential use as biological tracer agents.[6] The carbonylmetalloimmunoassay procedure is based on the IR stretching vibrations of organometallic carbonyl groups and has a sensitivity comparable with that of radioactive tracers.[6a] A second example is the use of metal carbonyls as carbon monoxide-releasing molecules.[7]

As indicated above, the primary way to control the properties of half-sandwich metal carbonyl compounds is to modify the steric, electronic and other properties of the first sphere ligands, for example the substituents on the Cp ring. A second approach involves introduction of a second-sphere ligand noncovalently attached to the first-sphere ligands. One of the most promising applications of this idea is the formation of inclusion compounds with cyclodextrins (CDs).[8] CDs and their derivatives are known to bind half-sandwich complexes such as $[CpFeX(CO)_2]$ (X = Cl, Me, CN),[9] $[CpFe(NH_3)(CO)_2](PF_6)$,[10] $[CpMn(CO)_3]$,[11] $[(\eta^6\text{-}C_6H_6)Cr(CO)_3]$,[12] $[CpMoX(CO)_3]$ (X = Cl, CH_2CONH_2),[9e,13] $[Cp'Mo(\eta^3\text{-}C_3H_5)(CO)_2]$,[14] $[Cp'Mo(\eta^3\text{-}C_6H_7)(CO)_2]$ and $[Cp'Mo(\eta^4\text{-}C_6H_8)(CO)_2](BF_4)$ (Cp′ = Cp, Ind).[15] Some of these encapsulated metallo-organic complexes exhibit markedly different physical and chemical characteristics in comparison with the bulk material. CD inclusion compounds are interesting for pharmaceutical use because of the enhanced solubility, stability and bioavailability of the drug molecules, as well as the reduced toxic

[a] Department of Chemistry, CICECO, University of Aveiro, 3810-193 Aveiro, Portugal
Fax: +351-234-370084
E-mail: igoncalves@dq.ua.pt
[b] Department of Chemistry, University of Cambridge, Lensfield Road, CB2 1EW Cambridge, United Kingdom

side-effects.[16] As part of an ongoing study aimed at improving the properties of potential organometallic pharmaceuticals by encapsulation in CDs, we now report on the encapsulation of the complexes $[CpMo(NCMe)_2(CO)_2](BF_4)$ and $[CpMo(H_2biim)(CO)_2](BF_4)$ (H_2biim = 2,2′-biimidazole) in β-CD and 2,3,6-tris-*O*-methyl-β-CD (TRIMEB). The molecular structures of the "free" dicarbonyl complexes have been determined by single-crystal X-ray diffraction and the inclusion compounds were characterised in the solid state by various techniques.

Results and Discussion

Preparation and Crystal Structures of the Molybdenum(II) Dicarbonyl Complexes

Treatment of $[CpMo(\eta^3\text{-}C_3H_5)(CO)_2]$ with $HBF_4{\cdot}Et_2O$ in dichloromethane affords the labile complex $[CpMo(\eta^2\text{-}C_3H_6)(CO)_2(FBF_3)]$,[17] which readily reacts with acetonitrile to give $[CpMo(NCMe)_2(CO)_2](BF_4)$ (**1**) and with 2,2′-biimidazole to give $[CpMo(H_2biim)(CO)_2](BF_4)$ (**2**) (Scheme 1). As expected, complexes **1** and **2** exhibit two ṽ(CO) stretching vibrations in their FTIR spectra, which can be attributed to the *cis*-$(CO)_2$ fragment. The bands for **2** (1976 and 1878 cm^{-1}) appear at lower frequencies than those for **1** (1988 and 1893 cm^{-1}) because H_2biim is a better electron donor (and acceptor) than acetonitrile and this results in higher Mo→CO back-donation and a weaker C≡O bond.

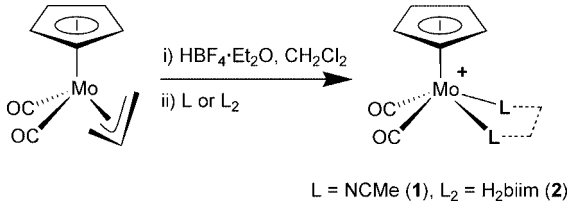

Scheme 1.

The crystal structures of compounds **1** and **2** were elucidated from single-crystal X-ray diffraction studies at low temperature (see Exp. Sect.) and show a number of striking similarities with respect to the geometries of the 18-electron half-sandwich molybdenum(II) cationic complexes and the crystal packing of each material.

Complex **1** crystallises in the orthorhombic *Pbca* space group with the asymmetric unit comprised of four individual residues (two metal complex cations plus two highly disordered tetrafluoroborate anions) and corresponding to the empirical formula $[CpMo(NCMe)_2(CO)_2](BF_4)$. Even though a great number of molybdenum complexes with η^5-cyclopentadienyl and carbonyl[18] or acetonitrile[19–26] ligands have been reported, only one structure containing the latter two ligands is known.[27] To the best of our knowledge, compound **1** represents the first complex containing all three of these ligands.

As often occurs for transition metal organometallic complexes, the structure of **1** contains two crystallographically independent $[CpMo(NCMe)_2(CO)_2]^+$ cations showing the same structural arrangement and rather similar coordination environments (Figure 1, Table 1). These coordination geometries can be envisaged as slightly distorted pseudo-square pyramids with the basal plane formed by two *cis*-coordinated carbonyl groups and two acetonitrile ligands and the apical position occupied by an η^5-coordinated cyclopentadienyl which, for clarity, is hereafter regarded as unidentate, with the coordination site being the centroid of the aromatic ring, C_g (Figure 1). This coordination geometry is commonly compared with a four-legged piano-stool[21] in which the metal centre emerges above the basal plane (ca. 0.92 and 0.93 Å for the two crystallographically independent complexes) leading to bond angles which deviate significantly from the ideal 90°. The Mo–C (carbonyl) and Mo–N bond lengths for the two complexes [1.967(4)–1.988(4) and 2.160(3)–2.179(3) Å, respectively] are in good agreement with those typically found in similar Mo/Cp complexes as revealed by a search of the Cambridge Structural Database (CSD) (Version 5.26, updated in August 2005).[28] Thus, while the typical Mo–C (carbonyl) bond lengths were found in the 1.64–2.37 Å range (from 1415 entries with a median of 1.97 Å), the Mo–N (acetonitrile) bond lengths are instead in the 2.12–2.20 Å range (from 16 entries with a median of 2.14 Å). Individual $Mo–C_{aromatic}$ bond lengths (Table 1) are also consistent with the values found in related compounds [2.12–2.74 Å for 2468 entries with a median of 2.34 Å]. However, as commonly encountered for complexes with the four-legged piano-stool resemblance,[29] the observed $Mo–C_{aromatic}$ bond lengths also indicate a slight "slip" from the expected η^5-coordination mode towards an η^3-type with the torsion angles between the planes defined by the Cp rings and the N···N···C···C bases of the pyramids being ca. 3.0 and 5.4° [for Mo(1) and Mo(2), respectively]. Indeed, the Mo–C(4,5) and Mo–C(13,14) bond lengths are statistically longer than the remaining distances within each Cp aromatic ring (Table 1). This structural feature is depicted in Figure 1 for one $[CpMo(NCMe)_2(CO)_2]^+$ complex cation. C(4) and C(5) are the closest atoms to the slightly bulkier acetonitrile ligands and the increase in the $Mo–C_{aromatic}$ bond length [$\Delta_{average}$(Mo–C) of ca. 0.09 Å with the largest being ca. 0.12 Å] presumably arises as the result of a tendency to reduce the steric pressure imposed upon the complex. The same occurs for the second complex cation but for atoms C(13) and C(14) instead [not represented – $\Delta_{average}$(Mo–C) and the largest bond length difference are identical to the values for the other complex].

Even though the coordination environments of the two crystallographically independent $[CpMo(NCMe)_2(CO)_2]^+$ cations show several similarities, a few geometric aspects of the square-pyramids are fundamentally different. As summarised in Table 1, the (N,C)–Mo–(N,C) bond angle ranges for the basal planes of the molybdenum square-pyramids are slightly distinct for the two complexes [76.60(10)–79.69(12)° and 74.57(15)–81.47(14)°], these differences arising from the way in which each crystallographically independent complex close-packs in the solid-state. Indeed, one

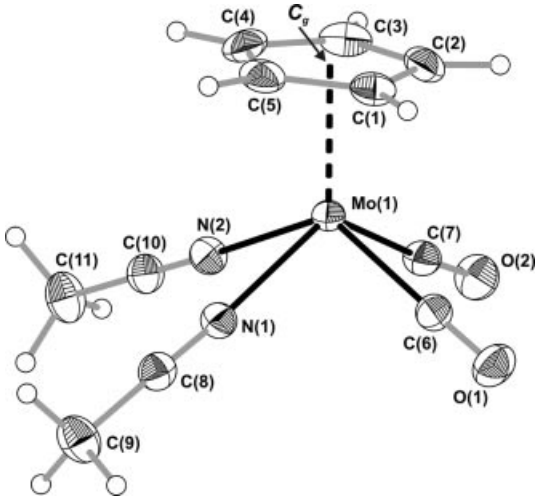

Figure 1. Schematic representation of one crystallographically independent $[CpMo(NCMe)_2(CO)_2]^+$ complex cation present in compound **1**, emphasising the slightly distorted square-pyramidal coordination environment for the Mo^{2+} metal centre and showing the labelling scheme for all non-hydrogen atoms. Displacement ellipsoids are shown at the 30% probability level and hydrogen atoms are represented as small spheres. All Mo–C bonds to the coordinated η^5-Cp have been omitted for clarity and replaced by a black-filled dashed bond line to the centroid, C_g. For selected bond lengths and angles see Table 1.

Table 1. Selected bond lengths [Å] and angles [°] for the molybdenum coordination environments of the two crystallographically independent $[CpMo(NCMe)_2(CO)_2]^+$ complex cations present in **1**.

Complex **1**			
Mo(1)–N(1)	2.164(3)	N(2)–Mo(1)–N(1)	76.60(10)
Mo(1)–N(2)	2.160(3)	C(6)–Mo(1)–N(1)	80.13(12)
Mo(1)–C(6)	1.988(4)	C(6)–Mo(1)–N(2)	128.58(12)
Mo(1)–C(7)	1.969(4)	C(7)–Mo(1)–N(1)	125.88(12)
Mo(1)–C(1)	2.299(3)	C(7)–Mo(1)–N(2)	79.69(12)
Mo(1)–C(2)	2.252(3)	C(7)–Mo(1)–C(6)	78.05(14)
Mo(1)–C(3)	2.272(3)	C_g–Mo(1)–C(6)	116.33(2)
Mo(1)–C(4)	2.352(3)	C_g–Mo(1)–C(7)	117.99(2)
Mo(1)–C(5)	2.369(3)	C_g–Mo(1)–N(1)	116.11(2)
Mo(1)–C_g[a]	1.977(1)	C_g–Mo(1)–N(2)	115.07(2)
Complex **2**			
Mo(2)–N(3)	2.179(3)	N(4)–Mo(2)–N(3)	76.96(11)
Mo(2)–N(4)	2.173(3)	C(17)–Mo(2)–N(3)	80.77(13)
Mo(2)–C(17)	1.967(4)	C(17)–Mo(2)–N(4)	125.91(12)
Mo(2)–C(18)	1.973(4)	C(17)–Mo(2)–C(18)	74.57(15)
Mo(2)–C(12)	2.286(4)	C(18)–Mo(2)–N(3)	127.73(12)
Mo(2)–C(13)	2.366(4)	C(18)–Mo(2)–N(4)	81.47(14)
Mo(2)–C(14)	2.367(4)	C_g–Mo(2)–C(17)	116.88(2)
Mo(2)–C(15)	2.284(4)	C_g–Mo(2)–C(18)	116.12(2)
Mo(2)–C(16)	2.248(3)	C_g–Mo(2)–N(3)	116.11(2)
Mo(2)–C_g	1.980(1)	C_g–Mo(2)–N(4)	117.20(2)

[a] C_g corresponds to the centroid of the coordinated η^5-Cp aromatic rings [C(1)–C(5) and C(12)–C(16)].

complex packs along the [100] direction of the unit cell in a typical interlocked head-to-head fashion, stabilised by π-π interactions between neighbouring η^5-Cp aromatic rings (distance of ca. 3.5 Å, Figure 2, a). Along this cationic chain the Mo(1)···Mo(1) distances alternate between 5.529(1) and 7.372(1) Å for head-to-head and tail-to-tail packing, respectively. However, the other crystallographically independent complex is instead distributed along the same direction in a head-to-tail fashion [see part c in Figure 2, Mo(2)···Mo(2) distance of 6.441(1) Å] which, in the absence of stabilising interactions between the aromatic ring and the carbonyl and/or acetonitrile moieties, leads to a slightly higher steric pressure on the basal plane, thus resulting in the increase of the (N,C)–Mo–(N,C) bond angles mentioned above.

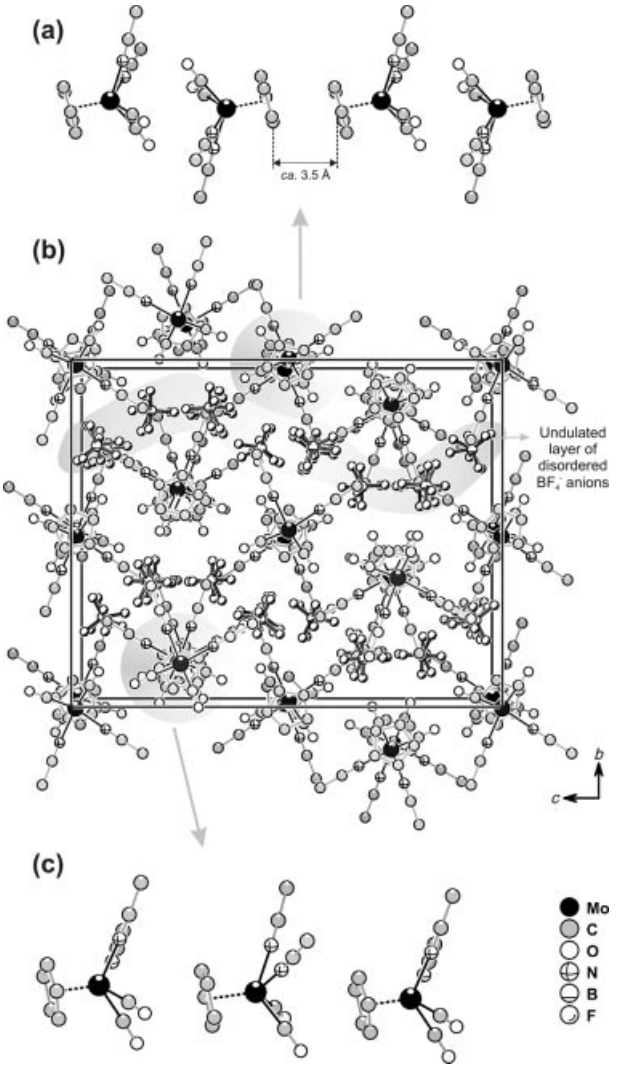

Figure 2. (a) Head-to-head-faced $[CpMo(NCMe)_2(CO)_2]^+$ complex cations in **1** distributed along the [100] direction, showing the π-π interactions between neighbouring η^5-Cp aromatic rings; (b) Crystal packing of **1** viewed in perspective along the [100] direction of the unit cell, emphasising the alternation in the [010] direction of undulated layers of $[CpMo(NCMe)_2(CO)_2]^+$ complex cations and BF_4^- anions; (c) Head-to-tail-faced $[CpMo(NCMe)_2(CO)_2]^+$ complex cations distributed along the [100] direction. Hydrogen atoms and Mo–C bonds to the coordinated η^5-Cp have been omitted for clarity.

The crystal packing of **1** is best described as the alternation along the [010] direction of the unit cell of undulated layers formed by the two crystallographically independent $[CpMo(NCMe)_2(CO)_2]^+$ cations with layers of disordered BF_4^- anions (Figure 2). Interactions between these moieties

are assured by a large number of weak C–H···F interactions (not shown).

The basic building unit of the complex [CpMo(H_2biim)(CO)$_2$](BF_4) (**2**) is the 18-electron half-sandwich [CpMo(H_2biim)(CO)$_2$]$^+$ cation, the molecular structure of which was first reported a few years ago by Romão and coworkers for [CpMo(H_2biim)(CO)$_2$]ReO_4 (**2R**).[30] Notably, that report still constitutes, to date, the only crystallographic study of a molybdenum complex with the chelating H_2biim ligand. Here we describe the second compound containing this complex cation, in which the tetraoxorhenium(VII) [ReO_4^-] moiety has been substituted by tetrafluoroborate anions and the crystal structure determined with increased precision and at low temperature (see Exp. Sect. for crystallographic details for the present study; **2R** was determined at ambient temperature with a very large R_1 reliability factor of 9.07%).

For compounds **2** and **2R**, the cation [CpMo(H_2biim)(CO)$_2$]$^+$ contains the molybdenum centre bound to a chelating H_2biim residue, two *cis*-coordinated carbonyl groups and an η^5-Cp moiety. The coordination geometry is, once again, best described as distorted square-pyramidal and very much resembles a four-legged piano-stool in which the base is formed by the chelating H_2biim and the carbonyl residues (Figure 3). The Mo–N and Mo–C (carbonyl) bond lengths are in agreement with those reported for **2R** and related compounds (Table 2). A search in the CSD for typical Mo–N distances of chelating ethanediimines shows values spanning from ca. 2.04 to 2.39 Å with a median of 2.24 Å (from 20 entries in the database). The bite angle of H_2biim to the Mo centres is comparable for the two complexes, being ca. 72.8° for **2R** and 72.6° for **2**.

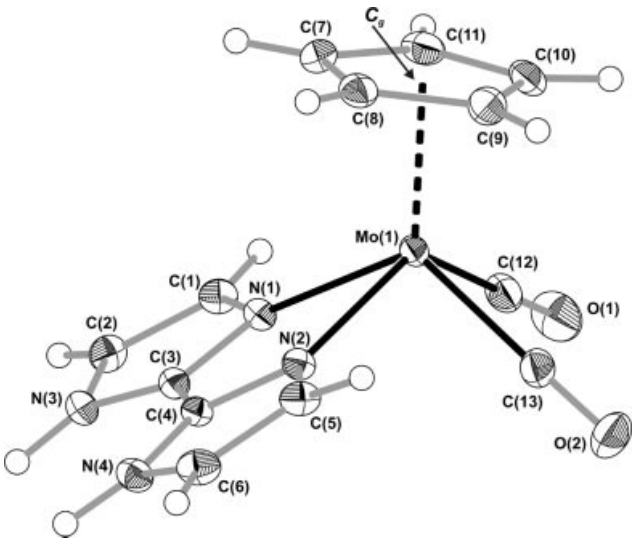

Figure 3. Schematic representation of the [CpMo(H_2biim)(CO)$_2$]$^+$ complex cation present in the crystal structure of **2**, emphasising the distorted square-pyramidal coordination environment for the Mo^{2+} metal centre and showing the labelling scheme for all non-hydrogen atoms. Displacement ellipsoids are drawn at the 30% probability level and hydrogen atoms are represented as small spheres. All Mo–C bonds to the coordinated η^5-Cp have been omitted for clarity and replaced by a black-filled dashed bond line to the centroid, C_g. For selected bond lengths and angles see Table 2.

Table 2. Selected bond lengths [Å] and angles [°] for the molybdenum coordination environment of the [CpMo(H_2biim)(CO)$_2$]$^+$ complex cation present in **2**.

Mo(1)–N(1)	2.189(2)	N(2)–Mo(1)–N(1)	72.55(8)
Mo(1)–N(2)	2.182(2)	C(12)–Mo(1)–N(1)	80.81(10)
Mo(1)–C(12)	1.981(3)	C(12)–Mo(1)–N(2)	130.11(9)
Mo(1)–C(13)	1.955(3)	C(13)–Mo(1)–N(1)	119.59(9)
Mo(1)–C(7)	2.381(3)	C(13)–Mo(1)–N(2)	80.89(9)
Mo(1)–C(8)	2.396(3)	C(13)–Mo(1)–C(12)	76.76(12)
Mo(1)–C(9)	2.313(3)	C_g–Mo(1)–C(12)	115.86(2)
Mo(1)–C(10)	2.265(3)	C_g–Mo(1)–C(13)	120.45(2)
Mo(1)–C(11)	2.296(3)	C_g–Mo(1)–N(1)	119.86(2)
Mo(1)–C_g[a]	1.996(1)	C_g–Mo(1)–N(2)	113.95(2)

[a] C_g corresponds to the centroid of the coordinated η^5-Cp aromatic ring [C(7)–C(11)].

By employing a much smaller anion (BF_4^-) to balance the charge of the Mo complex, the crystal packing driving forces mediated by hydrogen bonding interactions (see below) lead to a significant distortion of the geometry of the N···N···C···C base of the pyramid with observed *trans* angles of 130.11(9)° and 119.59(9)°. The corresponding values for **2R** are 124.9(10)° and 126.3(9)°. However, if we consider an average plane for the atoms forming this base, the displacement of the Mo centre towards the η^5-Cp moiety is ca. 0.96 Å, a value statistically identical to that observed for **2R** [0.94(1) Å]. The latter coordinated moiety is, once again, located at the apex of the distorted square-pyramid and also exhibits a deviation from the ideal η^5-coordination mode so as to release the steric repulsion with the H_2biim molecule. Indeed, compared with the acetonitrile molecules in compound **1**, the H_2biim molecule is bulkier and imposes statistically longer Mo–C(7,8) bonds [Table 2; $\Delta_{average}$(Mo–C) of ca. 0.07 Å with the largest being ca. 0.13 Å].

Individual [CpMo(H_2biim)(CO)$_2$]$^+$ cations close-pack in **2** along the [100] direction in a head-to-tail fashion (Figure 4, a) leading to a chain in which the minimum Mo···Mo separation is 6.531(2) Å. The crystal structure of **2** is formed by the alternation, in the [001] direction of the unit cell, of double layers of [CpMo(H_2biim)(CO)$_2$]$^+$ complex ions with BF_4^- anions. Interactions between these moieties are assured by strong N–H···F hydrogen bonds (see part b of Figure 4 and Table 3) and, as also reported for compound **1**, by a series of weak C–H···F interactions (not shown).

Table 3. Hydrogen bonding geometry (distances in Å and angles in °) for [CpMo(H_2biim)(CO)$_2$](BF_4) (**2**).[a]

D–H···A	*d*(D···A)	<(DHA)
N(3)–H(3)···F(4)^i	2.868(3)	144(3)
N(4)–H(4)···F(4)^i	3.116(3)	139(2)

[a] Symmetry transformation used to generate equivalent atoms: (i) $x-1, y, z$.

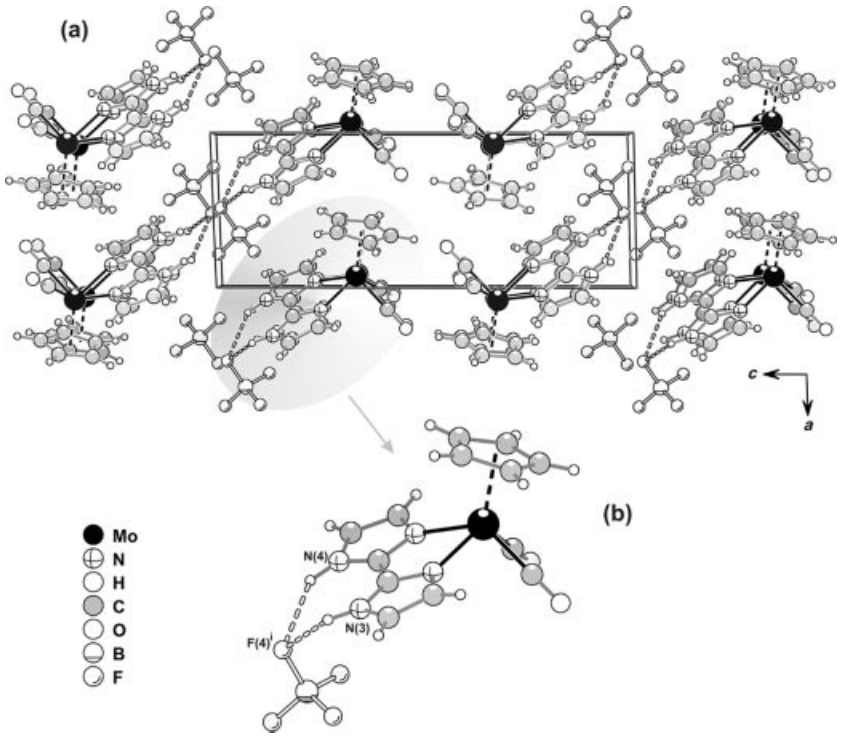

Figure 4. (a) Crystal packing of **2** viewed in perspective along the [010] direction of the unit cell; (b) Strong N–H···F hydrogen bonding interactions linking individual $[CpMo(H_2biim)(CO)_2]^+$ complex cations to neighbouring BF_4^- anions. For further details on the geometry of these interactions see Table 3. As in the previous schematic drawings, Mo–C bonds to the coordinated η^5-Cp moieties have been replaced by black-filled dashed bond lines to the centroid. Symmetry transformation used to generate equivalent atoms: (i) $x - 1, y, z$.

Cyclodextrin Inclusion Compounds

The relative solubilities of β-CD, TRIMEB and the complexes $[CpMo(NCMe)_2(CO)_2](BF_4)$ (**1**) and $[CpMo(H_2biim)(CO)_2](BF_4)$ (**2**) determined the method used for the preparation of the respective inclusion compounds. An initial CD/organometallic molar ratio of 1:1 was always used. For the preparation of β-CD·$[CpMo(NCMe)_2(CO)_2](BF_4)$ (**3**), an acetonitrile solution of **1** was added to an aqueous solution of β-CD, whereas for the preparation of β-CD·$[CpMo(H_2biim)(CO)_2](BF_4)$ (**5**) both components were dissolved in water. Compounds **3** and **5** were obtained as light brown and light brick coloured solids, respectively, after removal of the solvents by freeze-drying. The TRIMEB inclusion compounds TRIMEB·$[CpMo(NCMe)_2(CO)_2](BF_4)$ (**4**) and TRIMEB·$[CpMo(H_2biim)(CO)_2](BF_4)$ (**6**) were obtained by dissolving the components in either dichloromethane (**4**) or a mixture of dichloromethane and ethanol (**6**), followed by evaporation of the solvent(s) under reduced pressure.

X-ray diffraction studies enable the identification of true inclusion complexes of cyclodextrins, mainly based on the empirical evidence that the powder XRD patterns of these complexes should be clearly distinct from those obtained by the superimposition of the diffractograms of the individual components.[9e,31] Figure 5 shows the patterns for complexes **1** and **2**, plain β-CD hydrate, TRIMEB and the adducts **4** and **5**. The diffractograms of the adducts are clearly different from the sum of the individual patterns for complex **1** and TRIMEB, or complex **2** and β-CD. The TRIMEB adduct **4** is quite crystalline and the diffractogram shares similarities with the patterns exhibited by the corresponding 1:1 TRIMEB adducts of $[CpMoX(CO)_3]$ (X = Cl, CH_2CONH_2).[9e,13] A hypothetical structural model of the inclusion compound TRIMEB·$[CpMoCl(CO)_3]$ was obtained by global optimisation using simulated annealing.[9e] The compound crystallises in the space group $P2_12_12_1$ and the crystal packing features columns in which the macrocycles are arranged along the *b* axis in a tilted position. The TRIMEB inclusion compound **6** was found to be much less crystalline than **4**, exhibiting very broad and weak features at about 9.1, 11.5, 18.5 and 23.2° for 2θ in the powder XRD pattern (not shown). The β-CD adducts **3** and **5** had moderate crystallinity, with diffraction patterns very similar to that exhibited by the compound β-CD·$[CpMo(CH_2CONH_2)(CO)_3]$.[13]

Thermogravimetric analysis of compounds **3**–**6** was also useful for the recognition of inclusion complex formation. Figure 6 shows the TGA curves for $[CpMo(NCMe)_2(CO)_2](BF_4)$ (**1**), compounds **3** and **4**, and 1:1 physical mixtures of the pure hosts and complex **1**. Complex **1** features a weight loss of about 38% from 100 to 210 °C, which is in good agreement with the expected loss of 36% calculated for the removal of 2 NCMe and 2 CO ligands. A further gradual weight loss of 21% takes place up to 500 °C, leaving a residual mass of 38.2%. The first of these decomposition steps can be clearly seen in the TG profiles for the physical mixtures and is followed by the onset of cyclodextrin decomposition at about 270 °C for β-CD hydrate and

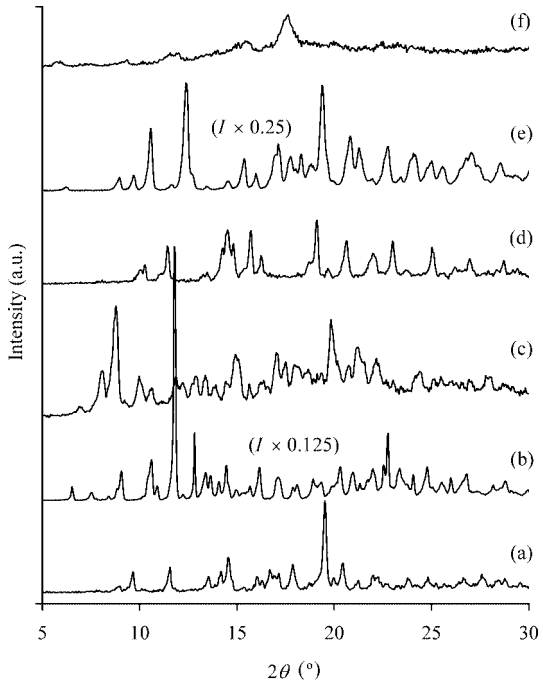

Figure 5. Powder XRD patterns of (a) $[CpMo(NCMe)_2(CO)_2](BF_4)$ (**1**), (b) TRIMEB, (c) the inclusion compound TRIMEB·$[CpMo(NCMe)_2(CO)_2](BF_4)$ (**4**), (d) $[CpMo(H_2biim)(CO)_2](BF_4)$ (**2**), (e) β-CD hydrate and (f) the inclusion compound β-CD·$[CpMo(H_2biim)(CO)_2](BF_4)$ (**5**).

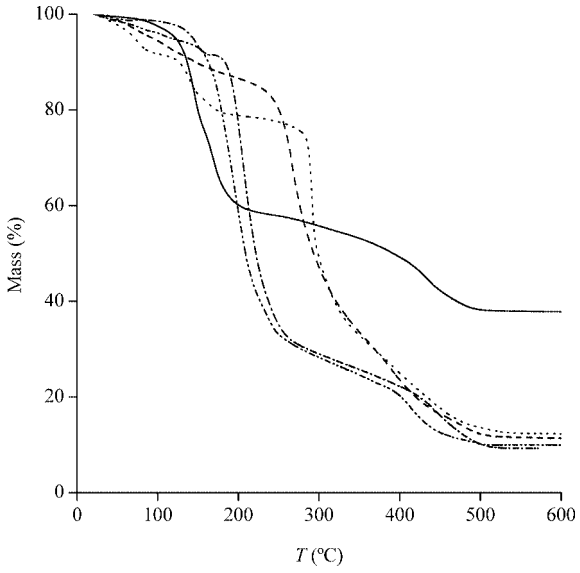

Figure 6. TGA curves of complex **1** (——), a 1:1 physical mixture of **1** and β-CD (·····), a 1:1 physical mixture of **1** and TRIMEB (–·–·) and the inclusion compounds **3** (– – –) and **4** (–··–··).

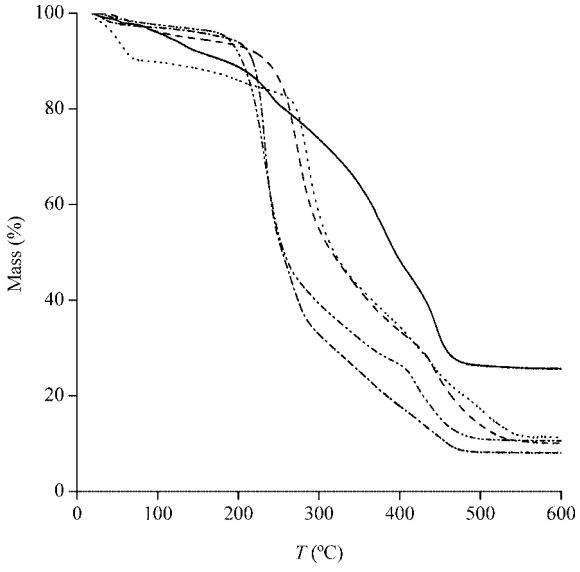

Figure 7. TGA curves of complex **2** (——), a 1:1 physical mixture of **2** and β-CD (·····), a 1:1 physical mixture of **2** and TRIMEB (–·–·) and the inclusion compounds **5** (– – –) and **6** (–··–··).

175 °C for TRIMEB. The TGA profile for the β-CD physical mixture exhibits an additional well-defined step from room temperature to 90 °C corresponding to the removal of water molecules located in the β-CD cavities and also in the interstices between the macrocycles. The TGA profiles for compounds **3** and **4** are very different from those for the physical mixtures. Neither individual steps for dehydration (in the case of the β-CD adduct) nor loss of the ligands from the organometallic complex were observed. Instead, both compounds exhibit a continuous and smooth weight loss from room temperature up to the points where the host macrocycles begin to decompose (230 °C for **3**, 155 °C for TRIMEB). This behaviour, coupled with the early degradation of the hosts (compared with the pure compounds β-CD hydrate and TRIMEB) is characteristic of true inclusion compounds comprising CDs and organometallic molecules. Comparable results were obtained for $[CpMo(H_2biim)(CO)_2](BF_4)$ (**2**) and its inclusion compounds (Figure 7), although the decomposition of the organometallic complex in the physical mixtures is not so obvious since the pure compound **2** decomposes in a series of overlapping steps which extend from room temperature to 475 °C.

The $^{13}C\{^1H\}$ CP/MAS NMR spectra of compounds **1**–**6** are shown in Figure 8 and Figure 9. Although the crystal structure of **1** contains two crystallographically independent $[CpMo(NCMe)_2(CO)_2]^+$ cations, with slightly different geometric features and distinct close-packing configurations, compound **1** gives rise to single peaks at 96.6, 145.1 and 252.6 ppm, assigned to the Cp, CN and CO groups, respectively. On the other hand, three partially revolved lines were observed between δ = 3 and 5 ppm for the methyl groups of the acetonitrile ligands. In the spectra of the inclusion compounds **3** and **4**, the guest species can be identified by a Cp resonance at about 96 ppm and a Me signal at about 3 ppm, which are essentially unshifted when compared with the resonances for nonincluded **1**. The β-CD carbon atoms in **3** give rise to four single peaks centred around 102.6, 80.6, 72.2 and 60.0 ppm, assigned to C1, C4, C2,3,5 and C6, respectively. This is in sharp contrast to plain β-CD hydrate, which exhibits a complex $^{13}C\{^1H\}$ CP/MAS NMR spectrum containing multiple sharp resonances for each type of carbon atom (not shown).[13] The multiple reso-

nances arise due to different torsion angles about the α(1→4) linkages[32] and the torsion angles describing the orientation of the hydroxy groups.[33] The appearance of single peaks in the $^{13}C\{^1H\}$ CP/MAS NMR spectrum of **3**, together with a lower dispersion in the chemical shift for each signal (i.e. the chemical shift range that comprises all of the resonances from the same carbon atom in distinct glycosidic units) are typically attributed to the β-CD macrocycle becoming symmetric, that is, the encapsulation of the guest molecule induces the ring to adopt a less distorted conformation, with each glucose unit in a more similar environment.[9e,13,34] The low crystallinity of compound **3** may also contribute to a broadening of the peaks.

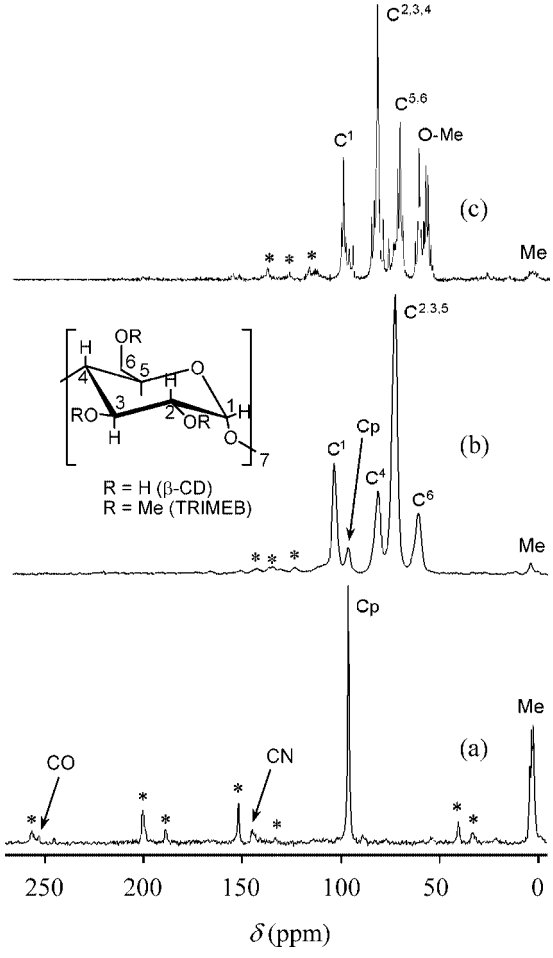

Figure 8. Solid-state $^{13}C\{^1H\}$ CP/MAS NMR spectra of (a) complex **1**, (b) the β-CD inclusion compound **3** and (c) the TRIMEB inclusion compound **4**. Spinning sidebands are denoted by asterisks.

Like plain β-CD hydrate, the $^{13}C\{^1H\}$ CP/MAS NMR spectrum of TRIMEB also contains multiple resonances for each type of carbon atom (not shown).[13] This is because the host assumes a severely collapsed conformation in the solid-state, which minimises the hydrophobic cavity in the absence of a hydrophobic guest.[35] Several resolved lines may also be observed for the inclusion compound **4** and this is consistent with the presence of an ordered crystal-packing arrangement of CD molecules. Indeed, the presence of at least ten sharp lines for the methyl carbon atoms shows that these groups exist in several different well-defined environments. The overall similarity of the spectrum with those previously reported for the adducts TRIMEB·[CpMoX(CO)$_3$] (X = Cl, CH_2CONH_2)[9e,13] is in line with the powder XRD results and confirms that the conformations of the host macrocycles and the crystal packing arrangements in the three compounds are similar. On the other hand, a comparison of these spectra with that for plain TRIMEB reveals considerable differences in the number, relative intensities and positions of peaks due to the host, which indicates that the conformation of the macrocycles in the inclusion compounds is different from that in plain TRIMEB.

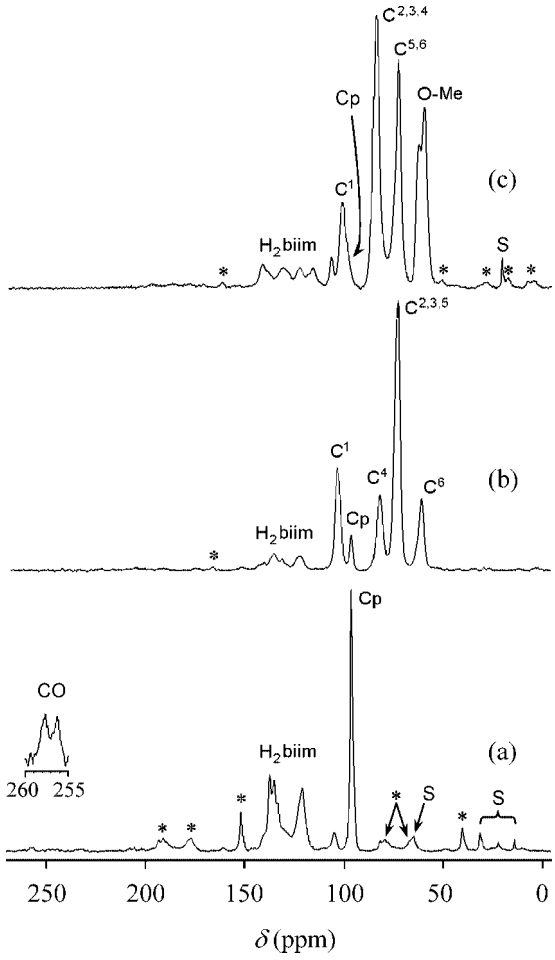

Figure 9. Solid-state $^{13}C\{^1H\}$ CP/MAS NMR spectra of (a) complex **2**, (b) the β-CD inclusion compound **5** and (c) the TRIMEB inclusion compound **6**. Spinning sidebands are denoted by asterisks and peaks due to the presence of residual solvents (diethyl ether, *n*-hexane or ethanol) are indicated by S.

Figure 9 shows the $^{13}C\{^1H\}$ CP/MAS NMR spectra of [CpMo(H_2biim)(CO)$_2$](BF$_4$) (**2**) and the inclusion compounds β-CD·[CpMo(H_2biim)(CO)$_2$](BF$_4$) (**5**) and TRIMEB·[CpMo(H_2biim)(CO)$_2$](BF$_4$) (**6**). The resonances for the carbon atoms of the biimidazole ligand in **2** appear in the range 120–137 ppm and the Cp resonance can be found at δ = 96.1 ppm. The spectrum for compound **5** is

very similar to that of compound **3** with respect to the β-CD carbon resonances. Additional peaks for the guest molecule can be observed at δ = 95.6 ppm (Cp) and 122–139 ppm (H_2biim). For the TRIMEB adduct **6**, the H_2biim resonances appear in the range of 115–140 ppm, while the Cp resonance is obscured by a broad peak for the C1 carbon atoms of the host. In fact, in contrast to the spectrum of **4**, the resonances for the host carbon atoms in **6** appear mainly as single broad peaks, which are presumably related to the low crystallinity of the compound as revealed by the powder XRD studies.

For all the inclusion compounds studied, it was not possible to clearly identify the resonances (masked in the background) for the CO groups of the guest molecules, even when contact times of 2 ms were used. The presence of these groups was confirmed by IR spectroscopy. Thus, in addition to the intense and typical bands of the cyclodextrin hosts, the spectra contained two bands in the CO stretching region (1880–2000 cm^{-1}). These were mostly shifted by less than 10 cm^{-1} compared with the corresponding bands for the nonincluded complexes **1** and **2**. Only in two cases (1971 cm^{-1} for **3** vs. 1988 cm^{-1} for **1**; 1891 cm^{-1} for **5** vs. 1878 cm^{-1} for **2**) were larger shifts observed. These shifts probably arise because the guest molecules in compounds **3**–**6** are isolated from one another by inclusion in the CD cavities.

Concluding Remarks

β-CD and TRIMEB inclusion compounds containing the complexes $[CpMo(NCMe)_2(CO)_2](BF_4)$ and $[CpMo(H_2biim)(CO)_2](BF_4)$ have been prepared and characterised. Referring to previous work, we may conclude that neutral, cationic or anionic η^5-cyclopentadienyl metal carbonyl complexes of the type $[CpML_m(CO)_n]^{z-/z+}$ (M = Mo, Mn or Fe), with three-legged or four-legged piano stool geometries, are readily encapsulated by cyclodextrins. The available experimental and theoretical evidence suggests that the interaction geometries generally involve insertion of the Cp ligand into the host cavities, with the CO and L ligands (L = NCMe, H_2biim, Cl, CH_2CONH_2 etc) protruding outwards (on the wider secondary side of the host molecules). Indeed, the crystal-packing arrangements in the β-CD and TRIMEB inclusion compounds containing the $[CpMo(NCMe)_2(CO)_2]^+$ complex cation are evidently very similar to the arrangements found in the corresponding inclusion compounds containing the neutral tricarbonyl complex $[CpMoCl(CO)_3]$. We are currently studying how the behaviour of the organometallic complexes as, for example, CO-releasing molecules, catalyst precursors or anti-tumour agents is affected by cyclodextrin encapsulation.

Experimental Section

General Remarks: All air-sensitive operations were carried out using standard Schlenk techniques under an oxygen- and water-free nitrogen atmosphere. Solvents were dried by standard procedures (diethyl ether and ethanol over Na, CH_2Cl_2 and NCMe over CaH_2), distilled under nitrogen and kept over 3 Å (NCMe) or 4-Å molecular sieves. Microanalyses for C, H and N were performed at the Instituto de Tecnologia Química e Biológica (Oeiras, Portugal) by C. Almeida and Mo was determined by ICP-OES at the Central Laboratory for Analysis (University of Aveiro) by E. Soares. TGA studies were carried out using a Shimadzu TGA-50 system at a heating rate of 5 °C min^{-1} under air. Powder X-ray diffraction data were collected at ambient temperature on a X′Pert MPD Philips diffractometer (Cu-K_α X-radiation, λ = 1.54060 Å) equipped with a curved graphite-monochromator and a flat-plate sample holder in a typical Bragg–Brentano *para*-focusing optics configuration (40 kV, 50 mA). Infrared spectra were recorded on a Unican Mattson Mod 7000 FTIR spectrometer. ^{13}C NMR spectra in solution were recorded on a Bruker Avance 500 spectrometer. $^{13}C\{^1H\}$ CP/MAS NMR spectra were recorded at 125.72 MHz on a (11.7 T) Bruker Avance 500 spectrometer, with an optimised $\pi/2$ pulse for ^1H of 4.5 μs, 2 ms contact time, a spinning rate of 7 kHz and 12 s recycle delays. Chemical shifts are quoted in parts per million relative to tetramethylsilane.

β-Cyclodextrin (Kleptose®) was kindly donated by laboratoires La Roquette (France) and heptakis-2,3,6-tris-*O*-methyl-β-CD was obtained from Fluka. 2,2′-Biimidazole was prepared from glyoxal and concentrated ammonia following the published method.[36] $[CpMo(\eta^3\text{-}C_3H_5)(CO)_2]$ was prepared as described in the literature[16b,16c] and characterised by elemental analysis and FTIR spectroscopy.

$[CpMo(NCMe)_2(CO)_2](BF_4)$ (1): A solution of $[CpMo(\eta^3\text{-}C_3H_5)(CO)_2]$ (0.35 g, 1.35 mmol) in CH_2Cl_2 was treated with 1 equiv. of $HBF_4{\cdot}Et_2O$. After 10 min, acetonitrile was added in excess and the reaction mixture was stirred for 2 h. The solution was then concentrated to about 5 mL and diethyl ether added to precipitate a red solid. The solid was filtered, washed with diethyl ether and *n*-hexane. Crystals suitable for X-ray analysis were obtained after slow diffusion at 4 °C of diethyl ether into a saturated solution of the crude product in acetonitrile. Yield: 0.48 g, 92%. $C_{11}H_{11}BF_4MoN_2O_2$ (385.96): calcd. C 34.23, N 7.26, H 2.87; found C 33.97, N 7.16, H 2.99. FTIR (KBr): $\tilde{\nu}$ = 3098 m, 3067 m, 3056 m (all ν_{CH} of Cp), 2972 m, 2965 m, 2915 m, 2902 m (all ν_{CH} of Me), 2325 w ($\nu_{N\equiv C}$), 2289 w ($\nu_{N\equiv C}$), 1988 vs. (ν_{CO}), 1893 vs. (ν_{CO}), 1621 m, 1434 m, 1422 m, 1366 w, 1352 w, 1305 w, 1300 w, 1083 vs. (ν_{BF}), 1073 s, 1036 s, 928 w, 904 vw, 886 vw, 869 vw, 847 m, 824 w, 772 vw, 713 vw, 588 m, 542 m, 533 m, 522 m, 513 m, 488 m, 458 m, 433 m, 385 m cm^{-1}. ^1H NMR (300 MHz, [D$_6$]acetone, 25 °C): δ = 5.80 (s, 5 H, Cp), 2.19 (s, 6 H, Me) ppm. $^{13}C\{^1H\}$ NMR (125.72 MHz, $CDCl_3$, 25 °C): δ = 249.7 (CO), 142.6 (CN), 96.1 (Cp), 4.8 (Me) ppm. $^{13}C\{^1H\}$ CP/MAS NMR: δ = 252.6 (CO), 145.1 (CN), 96.6 (Cp), 4.7 (Me) ppm

$[CpMo(H_2biim)(CO)_2](BF_4)$ (2): A solution of $[CpMo(\eta^3\text{-}C_3H_5)(CO)_2]$ (0.31 g, 1.19 mmol) in CH_2Cl_2 was treated with 1 equiv. of $HBF_4{\cdot}Et_2O$. After 10 min, dimethoxymethane was added in excess and the reaction mixture was stirred for 15 min. 2,2′-biimidazole (0.17 g, 1.30 mmol) was then added and the reaction mixture stirred for 4 h at room temperature. The resultant orange solution was filtered and, after concentrating to about 5 mL, diethyl ether was added to precipitate an orange microcrystalline solid. The solid was filtered and washed several times with diethyl ether and *n*-hexane. Crystals suitable for X-ray analysis were obtained after slow diffusion at 4 °C of diethyl ether into a saturated solution of the crude product in ethanol. Yield: 0.47 g, 90%. $C_{13}H_{11}BF_4MoN_4O_2$ (438.01): calcd. C 35.65, N 12.79, H 2.53; found C 35.52, N 12.51, H 2.38. FTIR (KBr): $\tilde{\nu}$ = 3360 s, br. (ν_{NH}),

3265 sh (ν_{NH}), 3156 m, 3140 s, 3122 s (ν_{NH}, ν_{CH} of Cp and/or H_2biim), 2929 m, 2776 m, 1976 vs. (ν_{CO}), 1878 vs. (ν_{CO}), 1707 w, 1638 m, 1534 m, 1512 m, 1429 m, 1420 m, 1359 w, 1321 m, 1284 w, 1253 w, 1123 s, 1100 s, 1068 vs. (ν_{BF}), 1004 m, 978 m, 919 w, 846 m, 822 m, 787 m, 761 s, 695 w, 679 m, 620 m, 612 w, 595 w, 538 m, 520 m, 484 m, 471 w, 435 m, 369 vw, 341 vw, 332 vw, 301 w cm^{-1}. ^{1}H NMR (300 MHz, [D$_6$]acetone, 25 °C): δ = 11.6 (NH, H_2biim), 7.75 (d, 2 H, H_2biim), 7.67 (d, 2 H, H_2biim), 5.85 (s, 5 H, Cp) ppm. ^{13}C{^{1}H} NMR (125.72 MHz, $CDCl_3$, 25 °C): δ = 253.0 (CO), 136.7, 133.9, 120.7 (all H_2biim), 95.2 (Cp) ppm. ^{13}C{^{1}H} CP/MAS NMR: δ = 257.6, 256.1 (CO), 137.3, 135.0, 133.3, 120.8 (all H_2biim), 104.8, 96.1 (Cp) ppm.

β-CD·[CpMo(NCMe)$_2$(CO)$_2$](BF$_4$) (3): A solution of [CpMo(NCMe)$_2$(CO)$_2$](BF$_4$) (**1**) (52.0 mg, 0.134 mmol) in acetonitrile (4.0 mL) was added to a solution of β-CD (152.5 mg, 0.134 mmol) in water (6.0 mL) at 40 °C. The resultant solution was stirred for 1 h and then frozen by immersion of the container in liquid nitrogen. The solvents were removed by freeze-drying to obtain a light-brown solid. FTIR (KBr): $\tilde{\nu}$ = 3375 s, br. (ν_{OH}), 2939 m, 1971 s (ν_{CO}), 1890 s (ν_{CO}), 1640 m, 1536 m, 1509 w, 1422 m, 1367 m, 1334 m, 1300 m, 1244 m, 1157 s, 1101 sh, 1079 vs, 1027 vs, 1003 sh, 946 m, 938 m, 892 w, 860 w, 829 w, 821 w, 762 m, 706 m, 698 m, 670 w, 608 m, 577 m, 527 m, 484 m, 432 m, 356 w, 327 w, 302 w cm^{-1}. ^{13}C{^{1}H} CP/MAS NMR: δ = 102.6 (β-CD, C1), 95.6 (guest Cp), 80.6 (β-CD, C4), 72.2 (β-CD, C2,3,5), 60.0 (β-CD, C6), 2.8 (guest Me) ppm.

TRIMEB·[CpMo(NCMe)$_2$(CO)$_2$](BF$_4$) (4): A solution of TRIMEB (0.558 g, 0.39 mmol) in CH_2Cl_2/water (20:1) was added to a solution of [CpMo(NCMe)$_2$(CO)$_2$](BF$_4$) (**1**) (103 mg, 0.26 mmol) in dichloromethane (10 mL) and the mixture was stirred for 48 h at 60 °C. After cooling to ambient temperature, the solution was evaporated to dryness under reduced pressure to obtain a dark-brown microcrystalline solid. FTIR (KBr): $\tilde{\nu}$ = 3463 s, 3106 m (ν_{CH} of Cp), 2989 s, 2935 s, 2842 s, 2322 vw ($\nu_{N\equiv C}$), 2290 vw ($\nu_{N\equiv C}$), 2074 w, 1988 s (ν_{CO}), 1944 w, 1899 s (ν_{CO}), 1840 w, 1631 m, 1458 m, 1384 m, 1370 m, 1325 m, 1307 m, 1263 m, 1196 s, 1163 s, 1145 s, 1107 vs, 1084 vs, 1072 vs, 1037 vs, 970 s, 951 m, 905 m, 856 m, 823 w, 805 w, 753 m, 734 m, 704 m, 671 vw, 553 m, 534 m, 522 m, 458 w, 434 w, 385 w, 348 w, 328 w, 313 w cm^{-1}. ^{13}C{^{1}H} CP/MAS NMR: δ = 100.5, 99.6, 99.2, 98.3 (TRIMEB, C1), 96.8, 96.5 (TRIMEB, C1; guest Cp), 94.7 (TRIMEB, C1), 85.4, 84.0, 82.4, 81.9, 81.3, 79.2 (TRIMEB, C2,3,4), 76.4, 74.2, 72.2, 71.0, 69.6 (TRIMEB, C5,6), 63.0, 61.8, 61.2, 60.0, 58.9, 58.1, 57.0, 56.5, 55.4 (TRIMEB, O–Me), 3.8 (guest Me) ppm.

β-CD·[CpMo(H$_2$biim)(CO)$_2$](BF$_4$) (5): A solution of β-CD (311 mg, 0.27 mmol) and [CpMo(H$_2$Biim)(CO)$_2$](BF$_4$) (**2**) (120 mg, 0.27 mmol) in water (8 mL) was stirred for 50 min at 50 °C and then frozen with liquid nitrogen. The frozen water was removed by liophilisation to obtain a brick-coloured solid. FTIR (KBr): $\tilde{\nu}$ = 3377 s, br. (ν_{OH}), 2928 m, 1973 s (ν_{CO}), 1891 s (ν_{CO}), 1640 m, 1534 m, 1507 w, 1422 m, 1368 m, 1334 m, 1300 w, 1245 w, 1157 s, 1099 sh, 1079 vs, 1050 sh, 1028 vs, 1005 sh, 944 m, 937 m, 861 w, 828 w, 820 w, 762 m, 706 m, 698 m, 668 m, 607 m, 577 m, 527 m, 483 m, 480 m, 433 m, 356 w, 335 w, 327 w, 302 w cm^{-1}. ^{13}C{^{1}H} CP/MAS NMR: δ = 139.2, 134.5, 130.2, 122.1 (all guest H_2biim), 102.5 (β-CD, C1), 95.6 (guest Cp), 80.7 (β-CD, C4), 71.9 (β-CD, C2,3,5), 59.8 (β-CD, C6) ppm.

TRIMEB·[CpMo(H$_2$biim)(CO)$_2$]BF$_4$ (6): A solution of [CpMo(H$_2$biim)(CO)$_2$]BF$_4$ (**2**) (60.0 mg, 0.137 mmol) in a mixture of dichloromethane (12 mL) and ethanol (4 mL) was treated portionwise with TRIMEB (196 mg, 0.137 mmol), allowing each fraction to dissolve before adding the next. The mixture was stirred for 1 h and then evaporated to dryness under reduced pressure to obtain a solid product. FTIR (KBr): $\tilde{\nu}$ = 3142 m (ν_{NH}, ν_{CH} of Cp and/or H_2biim), 2984 s, 2929 s, 2834 s, 2079 w, 1973 m (ν_{CO}), 1885 m (ν_{CO}), 1714 w, 1640 m, 1535 m, 1460 s, 1402 sh, 1369 m, 1322 m, 1304 m, 1259 sh, 1195 s, 1161 vs, 1141 vs, 1110 vs, 1095 vs, 1088 vs, 1072 vs, 1038 vs, 954 s, 937 s, 905 sh, 856 m, 821 w, 756 s, 706 m, 694 m, 666 w, 622 w, 599 sh, 551 m, 517 m, 468 w, 439 w, 377 vw, 346 w, 305 w cm^{-1}. ^{13}C{^{1}H} CP/MAS NMR: δ = 140.3, 129.7, 121.1, 115.0 (all guest H_2biim), 105.0, 99.5 (TRIMEB, C1; guest Cp), 82.2 (TRIMEB, C2,3,4), 71.1 (TRIMEB, C5,6), 60.6, 57.8 (TRIMEB, O–Me) ppm.

Single-Crystal X-ray Diffraction: Suitable single-crystals of [CpMo(NCMe)$_2$(CO)$_2$](BF$_4$) (**1**) and [CpMo(H$_2$Biim)(CO)$_2$](BF$_4$) (**2**) were mounted on glass fibres using perfluoropolyether oil.[37] Data were collected at 180(2) K on a Nonius Kappa charge-coupled device area-detector diffractometer (Mo-K_α graphite-monochromated radiation, λ = 0.7107 Å) equipped with an Oxford Cryosystems cryostream and controlled by the Collect software package.[38] Images were processed using the Denzo and Scalepack software packages[39] and data were corrected for absorption by the empirical method employed in Sortav.[40] Structures were solved by direct methods using SHELXS-97[41] and refined by full-matrix least-squares on F^2 using SHELXL-97.[42] All non-hydrogen atoms were directly located from difference Fourier maps and refined with anisotropic displacement parameters. Selected bond lengths and angles for the Mo^{2+} coordination environments are given in Table 1 and Table 2 for compounds **1** and **2**, respectively. Table 3 summarises the hydrogen bonding geometries reported for compound **2**.

For the two crystal structures, hydrogen atoms bound to carbon were located in their idealised positions using appropriate HFIX instructions in SHELXL (43 for the aromatic and 137 for the terminal methyl groups of the coordinated NCMe moieties) and included in subsequent refinement cycles in the riding-motion approximation with isotropic thermal displacement parameters (U_{iso}) fixed at 1.2 (for the aromatic hydrogen atoms) or 1.5 (for the methyl moieties) times U_{eq} of the carbon atom to which they were attached. For compound **1**, the two crystallographically independent BF_4^- anions were found to be severely affected by structural disorder, which was directly reflected in the large thermal displacement parameters calculated for each fluorine atom. This disorder was modelled by considering, on the one hand, two distinct crystallographic positions for each BF_4^- anion with fixed occupancy rates of $^1/_3$ and $^2/_3$ and, on the other, a geometry heavily restrained for each moiety with the B–F and F···F intramolecular distances restrained to variable common factors which ultimately refined to ca. 1.34 and 2.18 Å, respectively. This refinement strategy led to a more reasonable structural model for **1**, even though the checkCIF routines available with the PLATON software package still indicated a rather large discrepancy between the U_{eq} values of the boron and fluorine atoms. The last difference Fourier map synthesis showed, for **1**, the highest peak (0.535 e Å^{-3}) and deepest hole (–0.790 e Å^{-3}) located at 1.37 Å from H(20C) and 0.79 Å from Mo(1), respectively, while, for **2**, the highest peak (0.616 e Å^{-3}) and deepest hole (–0.798 e Å^{-3}) were found at 1.65 Å from H(3) and 0.79 Å from Mo(1), respectively.

CCDC-604073 and -604074 (for **1** and **2**) contain the supplementary crystallographic data for this paper. These data can be obtained free of charge from The Cambridge Crystallographic Data Centre via www.ccdc.cam.ac.uk/data_request/cif.

Crystallographic Data for 1: $C_{22}H_{22}B_2F_8Mo_2N_4O_4$, M = 771.94, orthorhombic *Pbca*, a = 12.871(3), b = 19.222(4), c = 23.849(5) Å, V = 5900(2) Å^3, Z = 8, $D_{calcd.}$ = 1.738 g cm^{-3}, μ(Mo-K_α) =

0.936 mm^{-1}, $F(000)$ = 3040, crystal size = 0.28 × 0.16 × 0.10 mm, brown blocks, θ range = 3.60 to 26.37, index ranges $-16 \le h \le 16$, $-17 \le k \le 24$, $-28 \le l \le 29$, reflections collected = 32704, independent reflections = 6001 (R_{int} = 0.0545), R_1, wR_2 [$I > 2\sigma(I)$] = 0.0345, 0.0739, R_1, wR_2 (all data) = 0.0513, 0.0803, weighting scheme m, n = 0.0330, 6.4200.

Crystallographic Data for 2: $C_{13}H_{11}BF_4MoN_4O_2$, M = 438.01, triclinic $P\bar{1}$, a = 6.5308(13), b = 7.2832(15), c = 16.962(3) Å, α = 92.91(3), β = 90.91(3), γ = 107.00(3)°, V = 770.2(3) $Å^3$, Z = 2, $D_{calcd.}$ = 1.889 $g\,cm^{-3}$, μ(Mo-K_α) = 0.912 mm^{-1}, $F(000)$ = 432, crystal size = 0.10 × 0.07 × 0.02 mm, red blocks, θ range = 3.51 to 30.03, index ranges $-9 \le h \le 9$, $-10 \le k \le 9$, $-23 \le l \le 23$, reflections collected = 10020, independent reflections = 4484 (R_{int} = 0.0406), R_1, wR_2 [$I > 2\sigma(I)$] = 0.0340, 0.0652, R_1, wR_2 (all data) = 0.0481, 0.0701, weighting scheme m, n = 0, 0.8582.

Acknowledgments

The authors are grateful to FCT, OE and FEDER for funding (Project POCI//QUI/56109/2004). CCLP is grateful to the FCT for a postdoctoral grant. We wish to thank Professor João Rocha for access to research facilities and Paula Esculcas for assistance in the solid-state NMR experiments. We are also grateful to Celeste Azevedo for carrying out the TGA experiments and to Rosário Soares for collection of the powder diffraction data.

[1] a) F. E. Kühn, A. M. Santos, W. A. Herrmann, *Dalton Trans.* **2005**, 2483–2491; b) A. A. Valente, J. D. Seixas, I. S. Gonçalves, M. Abrantes, M. Pillinger, C. C. Romão, *Catal. Lett.* **2005**, *101*, 127–130; c) J. Zhao, A. M. Santos, E. Herdtweck, F. E. Kühn, *J. Mol. Catal. A* **2004**, *222*, 265–271; d) B. F. M. Kimmich, P. J. Fagan, E. Hauptman, W. J. Marshall, R. M. Bullock, *Organometallics* **2005**, *24*, 6220–6229; e) Y. Kotani, M. Kamigaito, M. Sawamoto, *Macromolecules* **2000**, *33*, 3543–3549; f) O. Buisine, C. Aubert, M. Malacria, *Chem. Eur. J.* **2001**, *7*, 3517–3525; g) J. H. Hardesty, J. B. Koerner, T. A. Albright, G.-Y. Lee, *J. Am. Chem. Soc.* **1999**, *121*, 6055–6067.

[2] a) T. M. Gilbert, F. J. Hadley, C. B. Bauer, R. D. Rogers, *Organometallics* **1994**, *13*, 2024–2034; b) A. R. Dias, M. H. Garcia, M. P. Robalo, A. P. S. Tekheira, L. A. Bulygina, V. I. Sokolov, *Russ. J. Org. Chem.* **2001**, *37*, 620–623; c) M. H. Garcia, S. Royer, M. P. Robalo, A. R. Dias, J.-P. Tranchier, R. Chavignon, D. Prim, A. Auffrant, F. Rose-Munch, E. Rose, J. Vaissermann, A. Persoons, I. Asselberghs, *Eur. J. Inorg. Chem.* **2003**, 3895–3904.

[3] a) J. B. Waern, M. M. Harding, *J. Organomet. Chem.* **2004**, *689*, 4655–4668; b) R. H. Fish, G. Jaouen, *Organometallics* **2003**, *22*, 2166–2177; c) D. L. Mohler, E. K. Barnhardt, A. L. Hurley, *J. Org. Chem.* **2002**, *67*, 4982–4984.

[4] a) J. Bernard, K. Ortner, B. Spingler, H.-J. Pietzsch, R. Alberto, *Inorg. Chem.* **2003**, *42*, 1014–1022; b) M. Saidi, S. Seifert, M. Kretzschmar, R. Bergmann, H.-J. Pietzsch, *J. Organomet. Chem.* **2004**, *689*, 4739–4744.

[5] S. S. Braga, M. P. M. Marques, J. B. Sousa, M. Pillinger, J. J. C. Teixeira-Dias, I. S. Gonçalves, *J. Organomet. Chem.* **2005**, *690*, 2905–2912, and references therein.

[6] a) G. Jaouen, A. Vessières, I. S. Butler, *Acc. Chem. Res.* **1993**, *26*, 361–369; b) D. R. van Staveren, T. Weyhermüller, N. Metzler-Nolte, *Organometallics* **2000**, *19*, 3730–3735; c) J.-M. Heldt, N. Fischer-Durand, M. Salmain, A. Vessières, G. Jaouen, *J. Organomet. Chem.* **2004**, *689*, 4775–4782.

[7] a) T. R. Johnson, B. E. Mann, J. E. Clark, R. Foresti, C. J. Green, R. Motterlini, *Angew. Chem. Int. Ed.* **2003**, *42*, 3722–3729; b) I. J. S. Fairlamb, A.-K. Duhme-Klair, J. M. Lynam, B. E. Moulton, C. T. O'Brien, P. Sawle, J. Hammad, R. Motterlini, *Bioorg. Med. Chem. Lett.* **2006**, *16*, 995–998.

[8] a) F. Hapiot, S. Tilloy, E. Monflier, *Chem. Rev.* **2006**, *106*, 767–781; b) W. Sliwa, T. Girek, *Heterocycles* **2003**, *60*, 2147–2183; c) E. Fenyvesi, L. Szente, N. R. Russel, M. McNamara, in: *Comprehensive Supramolecular Chemistry*, (Eds.: J. Szejtli, T. Osa), Pergamon, Oxford, **1996**, vol. 3, pp. 305–366.

[9] a) M. Shimada, A. Harada, S. Takahashi, *J. Chem. Soc., Chem. Commun.* **1991**, 263–264; b) P. P. Patel, M. E. Welker, *J. Organomet. Chem.* **1997**, *547*, 103–112; c) C. Díaz, A. Arancibia, *J. Inclusion Phenom. Macro. Chem.* **1998**, *30*, 127–141; d) S. S. Braga, I. S. Gonçalves, P. Ribeiro-Claro, A. D. Lopes, M. Pillinger, J. J. C. Teixeira-Dias, J. Rocha, C. C. Romão, *Supramol. Chem.* **2002**, *14*, 359–366; e) S. S. Braga, F. A. Almeida Paz, M. Pillinger, J. D. Seixas, C. C. Romão, I. S. Gonçalves, *Eur. J. Inorg. Chem.* **2006**, 1662–1669.

[10] D. R. Alston, A. M. Z. Slawin, J. F. Stoddart, D. J. Williams, *Angew. Chem. Int. Ed. Engl.* **1985**, *24*, 786–787.

[11] L. Song, Q. Meng, X. You, *J. Organomet. Chem.* **1995**, *498*, C1–C5.

[12] A. Harada, K. Saeki, S. Takahashi, *Organometallics* **1989**, *8*, 730–733.

[13] S. S. Braga, S. Gago, J. D. Seixas, A. A. Valente, M. Pillinger, T. M. Santos, I. S. Gonçalves, C. C. Romão, *Inorg. Chim. Acta*, in press.

[14] S. S. Braga, I. S. Gonçalves, A. D. Lopes, M. Pillinger, J. Rocha, C. C. Romão, J. J. C. Teixeira-Dias, *J. Chem. Soc., Dalton Trans.* **2000**, 2964–2968.

[15] S. Lima, I. S. Gonçalves, P. Ribeiro-Claro, M. Pillinger, A. D. Lopes, P. Ferreira, J. J. C. Teixeira-Dias, J. Rocha, C. C. Romão, *Organometallics* **2001**, *20*, 2191–2197.

[16] a) T. Loftsson, M. E. Brewster, *J. Pharm. Sci.* **1996**, *85*, 1017–1025; b) R. A. Rajewski, V. J. Stella, *J. Pharm. Sci.* **1996**, *85*, 1142–1169.

[17] a) J. Markham, K. Menard, A. Cutler, *Inorg. Chem.* **1985**, *24*, 1581–1587; b) J. R. Ascenso, C. G. de Azevedo, I. S. Gonçalves, E. Herdtweck, D. S. Moreno, C. C. Romão, J. Zühlke, *Organometallics* **1994**, *13*, 429–431; c) J. R. Ascenso, C. G. de Azevedo, I. S. Gonçalves, E. Herdtweck, D. S. Moreno, M. Pessanha, C. C. Romão, *Organometallics* **1995**, *14*, 3901–3919.

[18] a) N. Begum, S. E. Kabir, G. M. G. Hossain, A. Rahman, E. Rosenberg, *Organometallics* **2005**, *24*, 266–271; b) C. M. Alvarez, M. A. Alvarez, M. E. Garcia, A. Ramos, M. A. Ruiz, M. Lanfranchi, A. Tiripicchio, *Organometallics* **2005**, *24*, 7–9; c) C. M. Alvarez, M. A. Alvarez, D. Garcia-Vivo, M. E. Garcia, M. A. Ruiz, D. Saez, L. R. Falvello, T. Soler, P. Herson, *Dalton Trans.* **2004**, 4168–4179; d) M. E. Garcia, V. Riera, M. A. Ruiz, D. Saez, J. Vaissermann, J. C. Jeffery, *J. Am. Chem. Soc.* **2002**, *124*, 14304–14305; e) I. P. Lorenz, S. von Beckerath, H. Noth, *Eur. J. Inorg. Chem.* **1998**, 645–650; f) M. Akita, K. Noda, Y. Takahashi, Y. Morooka, *Organometallics* **1995**, *14*, 5209–5220.

[19] A. J. Bridgeman, M. J. Mays, A. D. Woods, *Organometallics* **2001**, *20*, 2076–2087.

[20] P. Schollhammer, F. Y. Petillon, J. Talarmin, K. W. Muir, *Inorg. Chim. Acta* **1999**, *284*, 107–111.

[21] J. C. Fettinger, H.-B. Kraatz, R. Poli, E. A. Quadrelli, R. C. Torralba, *Organometallics* **1998**, *17*, 5767–5775.

[22] C. G. de Azevedo, M. J. Calhorda, M. Carrondo, A. R. Dias, M. T. Duarte, A. M. Galvão, C. A. Gamelas, I. S. Gonçalves, F. M. da Piedade, C. C. Romão, *J. Organomet. Chem.* **1997**, *544*, 257–276.

[23] A. Fries, M. Green, M. F. Mahon, T. D. McGrath, C. B. M. Nation, A. P. Walker, C. M. Woolhouse, *J. Chem. Soc., Dalton Trans.* **1996**, 4517–4532.

[24] C. Butters, N. Carr, R. J. Deeth, M. Green, S. M. Green, M. F. Mahon, *J. Chem. Soc., Dalton Trans.* **1996**, 2299–2308.

[25] J. C. Fettinger, D. W. Keogh, R. Poli, *J. Am. Chem. Soc.* **1996**, *118*, 3617–3625.

[26] G. R. Willey, T. J. Woodman, M. G. B. Drew, *J. Organomet. Chem.* **1996**, *510*, 213–217.

[27] H. Wadepohl, U. Arnold, H. Pritzkow, M. J. Calhorda, L. F. Veiros, *J. Organomet. Chem.* **1999**, *587*, 233–243.

[28] a) F. H. Allen, *Acta Crystallogr. Sect. B Struct. Sci.* **2002**, *58*, 380–388; b) F. H. Allen, W. D. S. Motherwell, *Acta Crystallogr. Sect. B Struct. Sci.* **2002**, *58*, 407–422.
[29] R. Poli, *J. Coord. Chem.* **1993**, *29*, 121–173.
[30] M. G. B. Drew, V. Felix, I. S. Gonçalves, F. E. Kühn, A. D. Lopes, C. C. Romão, *Polyhedron* **1998**, *17*, 1091–1102.
[31] W. Saenger, *Angew. Chem. Int. Ed. Engl.* **1980**, *19*, 344–362.
[32] a) M. J. Gidley, S. M. Bociek, *J. Am. Chem. Soc.* **1988**, *110*, 3820–3829; b) S. J. Heyes, N. J. Clayden, C. M. Dobson, *Carbohydr. Res.* **1992**, *233*, 1–14.
[33] R. P. Veregin, C. A. Fyfe, R. H. Marchessault, M. G. Tayler, *Carbohydr. Res.* **1987**, *160*, 41–56.
[34] L. Cunha-Silva, J. J. C. Teixeira-Dias, *New J. Chem.* **2005**, *29*, 1335–1341.
[35] G. R. Brown, M. R. Caira, L. R. Nassimbeni, B. van Oudtshoorn, *J. Inclusion Phenom. Macro. Chem.* **1996**, *26*, 281–294.
[36] a) M. J. Calhorda, A. R. Dias, *J. Organomet. Chem.* **1980**, *197*, 291–302; b) E. E. Bernarducci, P. K. Bharadwaj, R. A. Lalancette, K. Krogh-Jespersen, J. A. Potenza, H. J. Schugar, *Inorg. Chem.* **1983**, *22*, 3911–3920.
[37] T. Kottke, D. Stalke, *J. Appl. Crystallogr.* **1993**, *26*, 615–619.
[38] R. Hooft, *Collect: Data Collection Software*, Delft, The Netherlands, Nonius B. V., **1998**.
[39] Z. Otwinowski, W. Minor, in: *Methods in Enzymology*, Vol. 276 (Eds.: C. W. Carter Jr, R. M. Sweet), Academic Press, New York, **1997**, p. 307.
[40] a) R. H. Blessing, *Acta Crystallogr. Sect. A* **1995**, *51*, 33–38; b) R. H. Blessing, *J. Appl. Crystallogr.* **1997**, *30*, 421.
[41] G. M. Sheldrick, *SHELXS-97, Program for Crystal Structure Solution*, University of Göttingen, Germany, **1997**.
[42] G. M. Sheldrick, *SHELXL-97, Program for Crystal Structure Refinement*, University of Göttingen, Germany, **1997**.

Received: June 14, 2006
Published Online: September 18, 2006

